TECHNICAL TRANSACTIONS 4/2018
ELECTRICAL ENGINEERING
DOI: 10.4467/2353737XCT.18.058.8370
SUBMISSION OF THE FINAL VERSION: 25/3/2018

Volodymyr Samotyy (vsamotyy@pk.edu.pl)
Department of Automatic Control and Information Technology, Cracow University of Technology

Ulyana Dzelendzyak
Andriy Pavelchak
Department of Computer System and Automatic, Lviv Polytechnic National University, Ukraine

An evolutionary model for the parametric optimisation of electromagnetic instruments of variable structures

Model ewolucyjny optymalizacji parametrycznej urządzeń elektromagnetycznych o zmiennej strukturze

Abstract

This paper discusses the principle of constructing an evolutionary model for the parametric optimisation of electromagnetic instruments with solid-state valves. To illustrate the method, a triple voltage scheme was selected – this converts variable voltage into constant voltage and at the same time, triples the amplitude. Valve operation was modelled according to the ideal key diagram; the considered resistance was that of an open valve.

Keywords: evolutionary model, parametric optimisation, ideal key, voltage tripler, fixed mode, additional logic variables

Streszczenie

W pracy rozpatrzono zasady tworzenia modelu ewolucyjnego optymalizacji parametrycznej urządzeń elektromagnetycznych zawierających zawory półprzewodnikowe. Do ilustrowania metody wybraliśmy schemat przetwornicy napięcia zmiennego na stałe o potrójnej amplitudzie. Wykonuje on przetwarzanie napięcia zmiennego na stałe o trzykrotnej amplitudzie. Model diody wybieramy w postaci zawora idealnego. Przy czym jest uwzględniony jego opór w trybie otwartym.

Słowa kluczowe: model ewolucyjny, optymalizacja parametryczna, zawór idealny, przetwornica napięcia zmiennego na stałe o potrójnej amplitudzie, przebiegi ustalone, dodatkowe zmienne logiczne

1. Introduction

The conversion of voltage signal parameters is one of the most common forms of conversion in power electronics. This includes, inter alia, constant-to-variable, variable-to-constant, constant-to-constant and variable-to-variable voltage conversion. Another type of conversion worth mentioning is the change of output voltage amplitude with its galvanic distinction between input and output signals. Such converters are used in power supply units as modulators and also for the frequency control of electric motors. The devices which convert the constant voltage to variable voltage are called inverters, alternating current to direct current - rectifiers, direct current to direct current - converters, alternating current to alternating current - frequency converters.

The change of output voltage amplitude is performed by, for example, systems of rectifiers with multiplication of voltage (twofold, threefold, etc.). It should be noted that the base elements in the specified converters are variable-to-constant voltage converters and constant-to-variable voltage converters, i.e. rectifiers and inverters. Converters can be obtained directly by the linear connection of two converters, an inverter and a rectifier, whereas in frequency converters, their position should be switched – a rectifier should be placed on the input and an inverter on the output.

The use of mathematical modelling methods provides for development of mathematical models of voltage transducers. The bases of most mathematical models are the equations of the dynamics of the examined device. The compatibility of this solution to actual physical processes depending on how these equations correspond to the physics of the processes that take place in the voltage transducer.

Having written down the dynamics equation and the initial conditions of the state variables, the result is the Cauchy problem. Numerical methods of integration are used to solve the system of nonlinear differential equations because the task does not have an analytical solution. Integrating dynamics equations in a certain interval a transitional process settlement. If integration is performed with a fairly significant interval, it is possible to receive a fixed mode; however, it is never known in advance what that interval should be. So it is purposeful here to apply methods which have clear condition in entering the stationary mode. Such a condition is the persistence equation.

Analysis of transducers fixed work modes is a harder task than the settlement of transitional processes because it additionally requires the calculation of initial processes which meet the requirement for periodicity. The tested voltage transducers include both controlled and uncontrolled solid-state valves. Their volt-ampere properties feature high tortuosity when the valve crosses zero, which considerably hinders the modelling of their work modes. Two essentially different solid-state valve models exist. The first is based on the electric wheel theory with concentrated parameters, and the other model applies the magnetic field theory methods. The first model is divided into two further models; the first replaces the valve with the *RLC* link with variable parameters, and the other models it according to the ideal key diagram. In the first model, when the valve is open, the value of the active *R* link resistance is insignificant. When the voltage on the valve is negative, the received R resistance is quite high (hundreds of MOm). A risk of high overload is potentially present when comparably low valve

current is multiplied by its high resistance. To avoid this, the valve current crossing through zero must be determined. This considerably hinders the construction of the algorithm for numerical integration of dynamic equations.

The ideal key model leads to the appearance of a variable electric field structure – this means that the number of circuits and electric nodes changes depending on commutation. This has a direct effect on the voltage transducer dynamics equations. Every combination of open and closed valves is described with an algebraic-differential equations system. Such a situation is rather awkward because it requires going through different procedures depending on the execution of the conditions of valve opening and closing. It is proposed to introduce additional logical variables into dynamics equations which gain a value of 0, ±1. This allows the conversion of the entire system of equations into a single equation. These logical variables are components of the matrix elements of the dynamics equation coefficients and their values vary depending upon the conditions of the valve opening and closing.

Therefore, when constructing mathematical models of control system voltage transducers, one has to stick to the valve model according to the ideal key diagram using additional logical variables. This allows the description of the voltage transducers in the deferential equations modes. It must be noted that voltage transducers are widely used in automatics and control systems, observation systems, navigational systems, and in radio-electronics, etc. The existence of controlled and uncontrolled solid state valves in them makes it an extremely non-linear task; therefore, the issues solved in this paper are current and significant both in practical and theoretical terms.

2. Analysis of publications

A significant number of scientific works have been dedicated to voltage parameter transducers using solid state keys. A few of, were published in the last several years, will be considered below. A variable voltage regulator was examined in one of these pieces of work [1]. An attempt was made to approximate the form of the output signal to the sinusoid. The work of solid state keys was modelled by a changeover matrix – this means that non-linear valve features were not considered in the work. Whereas in [2], a single-phase current phase corrector was examined. A controller and PI regulator were used to control the device. A switching function was also used here for the modelling of valve diagrams. No analysis of parametric optimisation of the control process exists.

In work [3], width-impulse modulation was used to control the single-phase corrector. Realised transducer mathematical model acquired with the switching function. The control system was also examined in the violation of exploitation rules conditions. In work [4], a new triple-phased topology of an active rectifier was proposed. Such a topology lowers power losses in comparison to known diagrams of voltage rectification. Experimental studies were conducted in different exploitation conditions.

Very often, the thyristor voltage transducers lead to non-linear distortion in power supply networks. To eliminate such a phenomenon, the use of a configuration with many bridge

impulse transducers was proposed [5]. These are built using a transformer with multiple windings. Switching transistors often causes an overload that leads to them becoming damaged. In work [6], mild transistor switching was proposed – this eliminates the risk of an overload of the capacitor discharge by the transistor.

In work [7], power supply sources for illumination devices were examined – these are classic alternating-to-direct voltage impulse transducers (ac-dc). An asymmetric half-bridge was used here (AHB). The proposed methodology of applying AHB increases its effectiveness by as much as 94.5%. Model Predictive Control (MPC) [8] in thyristor voltage transducers in also known. Here, this was used for the two-level triple-phase transducer and compared with an array with similar approaches. In the examined examples of modelling the work of voltage transducers, open valve resistance in not considered. It is a non-linear valve current function. Furthermore, no analysis of the parametric optimisation of the work of voltage transducers exists. Our paper is dedicated to solving such tasks.

3. The dynamics equation of the voltage tripler

To illustrate the task, we will consider an alternating-to-direct voltage transducer with simultaneous amplitude tripling. It should be noted here that processing for such a type is possible if the load has high resistance (several kOm).

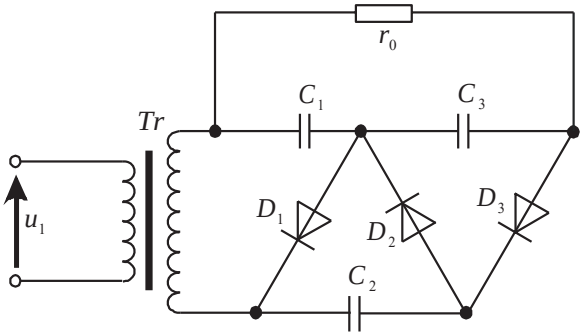

Fig. 1. Basic diagram of voltage tripler

A basic diagram of such voltage tripler is presented in Fig. 1. This includes a transformer (Tr), three diodes (D_1, D_2, D_3), three condensers (C_1, C_2, C_3) and load (r_O). In the positive wave, the condenser C_1 is loaded to the amplitude of the output voltage of the transformer. In the negative wave, the condenser C_2 is loaded up to double the condenser voltage C_1. This cycle is ended with the condenser charging up to C_3 double the condenser voltage C_1. When voltage is added on condensers C_1 and C_3, the result is triple voltage on the load r_0.

When formulating the dynamics equations, the parameters of the primary side of the transformer must be considered led to the secondary side, due to the number of coils, and the operation of solid state valves will be presented according to the ideal key diagram. The notion of 'ideal' will be understood as a key in which resistance in the closed condition is limitless and in the

open condition, it is constant, e.g. equal to zero. The idea of construction of mathematical models of such instruments consists of such an algorithm. First, it is necessary to explain the possible number of combinations of open and closed valves – for each of these, their own algebraic-differential equation system must be provided. Their common features must be determined and, using additional logical variables, a single genera system of equations must be formulated.

This allows the obtaining of four possible combinations of open and closed valves in the given diagram: 1) D_1 – open, D_2, D_3 – closed; 2) D_2 – open, D_1, D_3 – closed; 3) D_3 – open, D_1, D_2 – closed; 4) D_1, D_2, D_3 – closed.

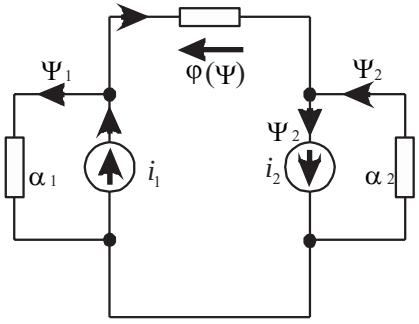

Fig. 2. Calculation of transformer magnetic field

Let us consider the dynamics equations for the first combination of the valve condition. In order to formulate these, we need the diagrams of change of the electric and magnetic field of the tripler. Calculation of the magnetic field is presented in Fig. 2 and for the electric winding circuits – Fig. 3. The proper equations for the calculation of the magnetic field (Fig. 2) are as follows:

$$\Psi_1 = \psi_1 + \psi, \quad \Psi_2 = \psi_2 + \psi, \tag{1}$$

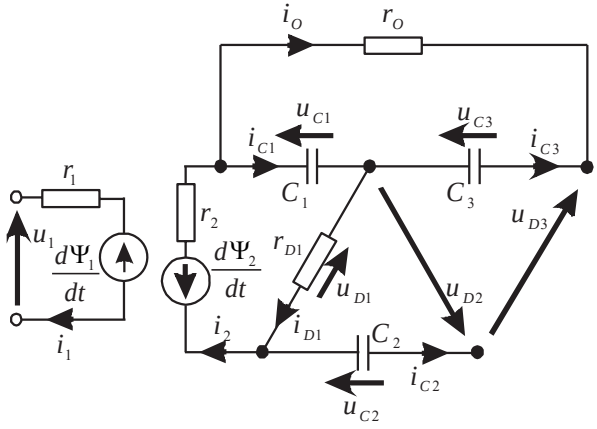

Fig. 3. Calculation of transformer electrical circuits

where ψ_1, ψ_2 – coupled coil dispersion streams; ψ – main steam coupling. Both here and further in this paper, the indices '1' and '2' indicate a connection with the primary and secondary winding of the transformer.

For dispersion systems (Fig. 2) the resulting equation is

$$i_1 = \psi_1 \alpha_1, \quad i_2 = \psi_2 \alpha_2, \tag{2}$$

where α_1, α_2, i_1, i_2 – values replaced with inductivity of dispersion and current of the winding.

Let us substitute (2) with (1) and determine the transformer winding current

$$i_1 = \alpha_1(\Psi_1 - \psi), \quad i_2 = \alpha_2(\Psi_2 - \psi). \tag{3}$$

According to the second Kirchhoff's law, for the magnetic field (Fig. 2), the equation is

$$i_1 + i_2 = \phi(\psi), \tag{4}$$

where $\varphi(\psi)$ – transformer core magnetising curve.

The transformer winding equations according to the calculation in Fig. 3 are as follows:

$$\frac{d\Psi_1}{dt} = u_1 - r_1 i_1, \quad \frac{d\Psi_2}{dt} = -u_{C1} - r_2 i_2 - u_{D1}, \tag{5}$$

where Ψ_1, Ψ_2, r_1, r_2 – full coupling of streams and resistance of transformer winding; u_1, u_{C1} – power supply and condenser voltage C_1.

Calculating the time derivative from equations (3) and (4) will give the result regarding the time derivative of the basic coupling

$$\frac{d\psi}{dt} = g_1 \frac{d\Psi_1}{dt} + g_2 \frac{d\Psi_2}{dt}, \quad g_1 = \frac{\alpha_1}{\alpha'' + \alpha_1 + \alpha_2}, \quad g_2 = \frac{\alpha_2}{\alpha'' + \alpha_1 + \alpha_2}. \tag{6}$$

Let us calculate the time derivative of the second equation (3) and enter (6) in the obtained equation result

$$\frac{di_2}{dt} = a_{21} \frac{d\Psi_1}{dt} + a_{22} \frac{d\Psi_2}{dt}, \quad a_{21} = -\alpha_2 g_1, \quad a_{22} = \alpha_2(1 - g_2). \tag{7}$$

The primary winding current must be determined analytically, according to (4)

$$i_1 = \phi(\psi) - i_2. \tag{8}$$

The obtained equations must be supplemented with condenser equations

$$\frac{du_{C1}}{dt} = \left(i_2 - \frac{u_{C1} + u_{C3}}{r_O} \right) / C_1, \quad \frac{du_{C2}}{dt} = 0, \quad \frac{du_{C3}}{dt} = -\frac{u_{C1} + u_{C3}}{r_O C_3} \tag{9}$$

where r_O – load resistance.

The load current must be calculated according to the following formula:

$$i_O = (u_{C1} + u_{C3}) / r_O \,. \tag{10}$$

Valve D_1 closed under condition

$$i_{D1} = i_2 \le 0 \,. \tag{11}$$

Let us consider the dynamics equations for the second combination of the valve condition. The calculation of the winding electrical circuits is presented in Fig. 4. The transformer equation remains unchanged, except for the second equation (5)

$$\frac{d\Psi_2}{dt} = -u_{C1} - r_2 i_2 + u_{C2} + u_{D2} \tag{12}$$

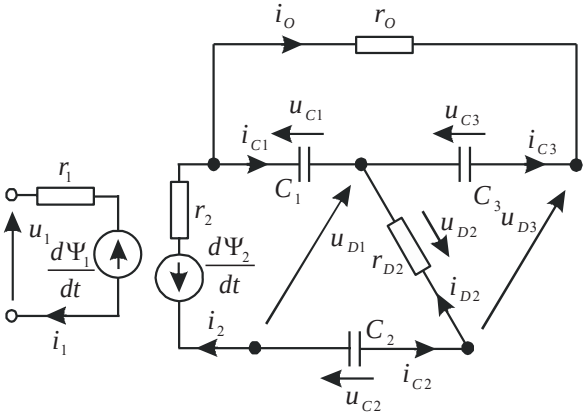

Fig. 4. Calculation of transformer electrical circuits

The condenser equations will assume the following form:

$$\frac{du_{C1}}{dt} = \left(i_2 - \frac{u_{C1} + u_{C3}}{r_O} \right) / C_1 , \quad \frac{du_{C2}}{dt} = -i_2 / C_2 , \quad \frac{du_{C3}}{dt} = -\frac{u_{C1} + u_{C3}}{r_O C_3} \tag{13}$$

Valve D_2 closed under condition

$$i_{D2} = -i_2 \le 0, \ \rightarrow \ i_2 \ge 0 \,. \tag{14}$$

Now, let us consider the dynamics equations of the third valve combination condition. Calculation of the electrical circuits is presented in Fig. 5. The transformer equations remain unchanged, except for the second equation (5)

$$\frac{d\Psi_2}{dt} = -u_{C1} - r_2 i_2 + u_{C2} - u_{C3} - u_{D3} \tag{15}$$

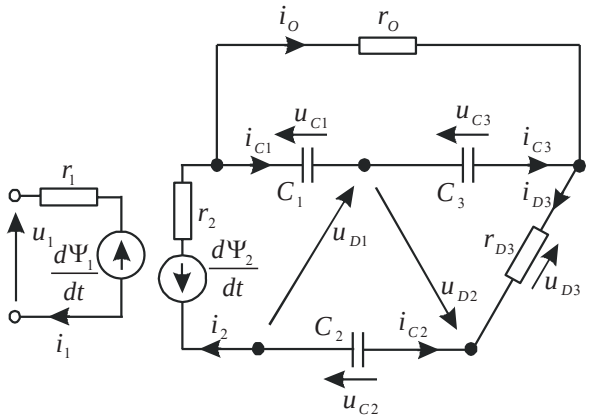

Fig. 5. Calculation of transformer electrical circuits

The condenser equations assume the following form:

$$\frac{du_{C1}}{dt}=\left(i_2-\frac{u_{C1}+u_{C3}}{r_O}\right)/C_1,\quad \frac{du_{C2}}{dt}=-i_2/C_2,\quad \frac{du_{C3}}{dt}=\left(i_2-\frac{u_{C1}+u_{C3}}{r_O}\right)/C_3. \tag{16}$$

Valve D_3 is closed under condition

$$i_{D3}=i_2\le 0. \tag{17}$$

Let us consider the dynamics equations for the fourth combination of the valve condition. The calculation of winding electrical circuits is presented in Fig. 6. When all valves are closed, the transformer is disconnected from load (i_2=0). For this reason, equations change, namely:

$$\frac{d\psi}{dt}=g_1\frac{d\Psi_1}{dt},\quad g_1=\frac{\alpha_1}{\alpha''+\alpha_1}. \tag{18}$$

$$\frac{d\Psi_2}{dt}=\frac{d\psi}{dt}. \tag{19}$$

$$\frac{di_2}{dt}=0. \tag{20}$$

The capacitor equations will take the following form:

$$\frac{du_{C1}}{dt}=-\frac{u_{C1}+u_{C3}}{r_OC_1},\quad \frac{du_{C2}}{dt}=0,\quad \frac{du_{C3}}{dt}=-\frac{u_{C1}+u_{C3}}{r_OC_3}. \tag{21}$$

These equations must be filled in with conditions for opening valves

$$u_{D1}=-u_{C1}-\frac{d\psi}{dt}>u_{open}=0, \tag{22}$$

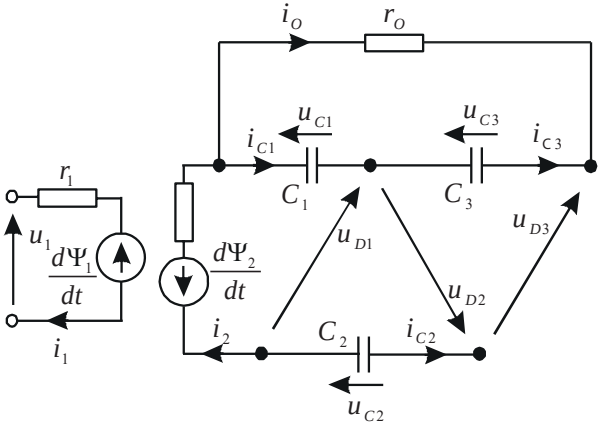

Fig. 6. Calculation of transformer electrical circuits

$$u_{D2} = u_{C1} - u_{C2} + \frac{d\psi}{dt} > u_{open} = 0, \tag{23}$$

$$u_{D3} = -u_{C1} + u_{C2} - u_{C3} - \frac{d\psi}{dt} > u_{open} = 0, \tag{24}$$

Let us introduce additional logical variables k_1, k_2, k_3 which take value 0 when the valve is closed and value 1 when it is open. When, upon fulfilment of condition (22), the variable k_1 takes value 1, upon fulfilment of condition (23) k_2=1, upon fulfilment of condition (24) k_3=1. Whereas, upon fulfilment of condition (11) k_1=0, upon fulfilment of condition (14) k_2=0, upon fulfilment of condition (17) k_3=0.

The result of the above is four different equation systems for each combination of valve status. Upon comparison and application of the additional logical variable, it is possible to narrow it down to the following system:

$$\frac{d\psi}{dt} = g_1 \frac{d\Psi_1}{dt} + g_2 \frac{d\Psi_2}{dt}, \; g_1 = \frac{\alpha_1}{\alpha'' + \alpha_1 + k\alpha_2}, \; g_2 = \frac{k\alpha_2}{\alpha'' + \alpha_1 + k\alpha_2}, \tag{25}$$

$$\frac{di_2}{dt} = a_{21} \frac{d\Psi_1}{dt} + a_{22} \frac{d\Psi_2}{dt}, \; a_{21} = -k\alpha_2 g_1, \; a_{22} = k\alpha_2 (1 - g_2), \tag{26}$$

$$\frac{du_{C1}}{dt} = \left(ki_2 - \frac{u_{C1} + u_{C3}}{r_O} \right) / C_1, \tag{27}$$

$$\frac{du_{C2}}{dt} = -(k_2 + k_3) i_2 / C_2, \tag{28}$$

$$\frac{du_{C3}}{dt} = \left(k_3 i_2 - \frac{u_{C1} + u_{C3}}{r_O} \right) / C_3, \tag{29}$$

$$\frac{d\Psi_1}{dt} = u_1 - r_1 i_1, \quad \frac{d\Psi_2}{dt} = -u_{C1} + (1-k_1)u_{C2} - k_3 u_{C3} - r_2 i_2 + u_D, \tag{30}$$

where $k = k_1 + k_2 + k_3$, $u_D = -k_1 u_{D1} + k_2 u_{D2} - k_3 u_{D3}$.

4. Results of the voltage tripler modelling

A program in C# language was prepared for the mathematical modelling of the device and simulation of its dynamic processes was performed.

One-phase voltage of the transformer power supply was set with the formula

$$u_1 = U_m \sin(2\pi f t), \tag{31}$$

where U_m = 311 V, f = 50 Hz.

The calculations of the mathematical model were conducted with the following device parameters values: $r_1 = r_2 = 0.1\ \Omega$; $r_O = 9000\Omega$; $\alpha_1 = 100\text{H}^{-1}$; $\alpha_2 = 200\text{H}^{-1}$; $C_1 = 40\mu\text{F}$; $C_2 = 600\mu\text{F}$; $C_1 = 400\mu\text{F}$. The magnetisation curve is approximated by formula (32).

$$\phi(\psi) = \begin{cases} m_1\psi & if\ |\psi| > \psi_1 \\ S_3(\psi) & if\ \psi_1 \le |\psi| \le \psi_2 \\ m_2\psi - m_0 & if\ |\psi| > \psi_2 \end{cases} \tag{32}$$

where m_1 = 0.25 H^{-1}; m_2 = 3 H^{-1}; a_0 = 1.8 A; ψ_1 =0.2 Wb; ψ_2 =0.9 Wb; $\varphi(\psi_1)$ = 0.05 A; $\varphi(\psi_2)$ = 0.09 A; $S_3(\psi)$ – cubic spline.

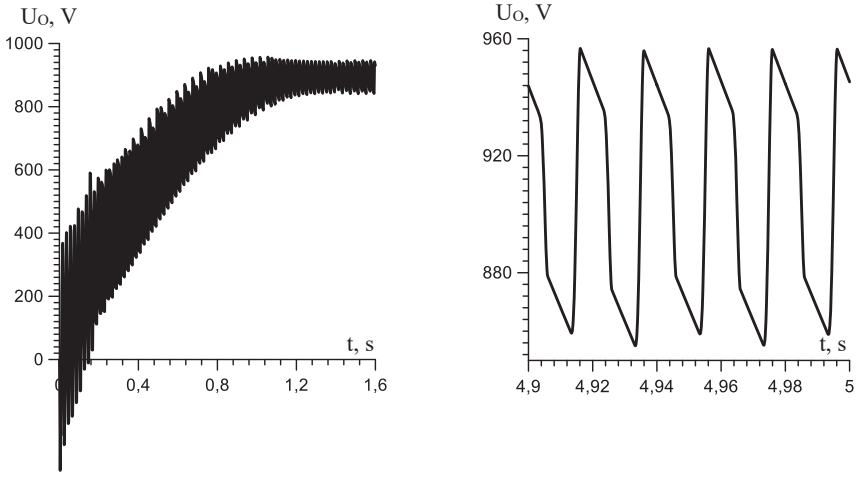

Fig. 7. Transient response of the voltage tripler

Fig. 7 presents the results of simulation of our voltage tripler. The device really triples our input voltage; however, with selected capacitor parameters, very high pulsations of input voltage in the range of 105 V are observed. In order to improve the output specification of the device, it is necessary to perform the optimisation for capacitor parameters.

Table 1 shows the values of volt-ampere specification for diode S1M.

Table 1. Table 1. The voltage-ampere specification of diode S1M at 25 °C

I_F, A	U_F, V	Rd, Ω
0.01	0.67	67
0.1	0.78	7.8
1	0.97	0.97
10	1.41	0.141

The other issue we were interested in was the impact of non-linear diode resistances on the mathematical model. In our model of the device, the applied model was the model of ideal key for diodes. For this reason, an additional test concerning the impact of the diode model on the final results was performed.

The function of dependency of resistance on the current of diode S1M was approximated with the formula

$$R_D(i_D)=\begin{cases} R_{D\max} & if\ |i_D| \le I_{D\min} \\ 1.0393\cdot i_D^{-0.8936} & if\ I_{D\min} < |i_D| < I_{D\max} \\ R_{D\min} & if\ |i_D| \ge I_{D\max} \end{cases} \tag{33}$$

where $R_{D\max} = 67\ \Omega$; $R_{D\min} = 0.141\ \Omega$; $I_{D\max} = 10\ A$; $I_{D\min} = 0.01\ A$.

The mathematical model was considered the threshold of the voltage of opening diodes which is applied in formulas (22–24) with determination $u_{open} = 0.67\ V$. In the equations of resistance dynamics, diodes R_D are systematically switched off with resistance r_2 and $i_D = i_2$. In the case of the modelling performed with consideration to the diode model, the qualitative specification of the device did not change – numeral changes in the output signal in the set mode were present in the five-digit series (maximum and minimum amplitude was registered).

5. Results of the voltage tripler optimisation

The selection of the parameter values of the voltage tripler was performed with the use of a classical genetic algorithm with the representation of genes with real digits [10, 11]. At performance, certain capability assumed for the genetic algorithm: to suspend/renew algorithm operation, possibility to change algorithm settings in the suspension mode (selection of

numeral population, number of generations, selection of method of pairing, selection, crossing, mutation, change of likelihood of gene mutation, elitism settings); it was foreseen that there could be a possibility to maintain transitional data of the search for optimum solution with parameters set for the genetic algorithm and continue the search from the maintained point.

The device parameters should be harmonised in the range [0, 1] for the genetic algorithm. Coding the parameters of the tested device with genes and reverse decoding is performed according to formulas (34)

$$gene_i = \frac{param_i - valueMin_i}{valueMax_i - valueMin_i} \tag{34}$$

$$param_i = valueMin_i + gene_i \cdot \left(valueMax_i - valueMin_i\right)$$

In our performance of the genetic algorithm, the initial population is generated in a random manner in harmonised ranges [0, 1]. The selection of individuals in a population is performed with linear ranking

$$Fitne\beta(Pos) = 2 - SP + 2 \cdot (SP - 1) \cdot \frac{Pos - 1}{Nind - 1} \tag{35}$$

where *Pos* – position of individuals in the population (the least adapted individuals have *Pos* = 1; the best adapted have *Pos* = *Nind*), *Nind* – quantity of individuals in the population, *SP* – co-efficient of selection impact can be significant in the range [1.0; 2.0]. According to value Fitneβ, the quantity of individual entries in the population is determined.

While pairing individuals, two operators were applied: «better with better» and «better with worse». At the beginning, we used operator «better with better» and at the end of the search for the optimum solution at the introduction of the population, we used operator «better with worse».

For crossing, the operator which imitates one-point binary crossing [11] was used. For mutation, operator Uniform was used.

The performance of the genetic algorithm was performed in C# language. An in-built generator of pseudo-random numbers with the principle of even distribution was used to generate random values which were built on the basis of the subtraction algorithm of random numbers developed by D. Knuth. The calculations of fitness value (adaptation function) for individuals separate depending on the existence of quantity of physical (logical) cores of the PC processor.

For the optimisation of the dynamic specification of the voltage tripler, the aforementioned genetic algorithm was applied.

The condenser values not only have an effect on the pulse size of the output signal, they also change its periodicity. Therefore, the method for accelerated switching into the fixed mode was not used, and for the purpose of search for the optimum solution, the end section of the transitional process was used.

Integrating current dynamics equations was performed in the time interval of T = 5 seconds. As a criterion for the fitness function value, we selected the impulse value of the output voltage at 0.9·T. This means that the fitness values were calculated according to the following formula:

$$Fitness = U_{O\max} - U_{O\min}$$
$$\text{if } (U_{O\min} < 850) \quad \text{then:} \quad Fitness = Fitness + 850 - U_{O\min} \tag{36}$$

When calculating the fitness value (36), an additional condition was introduced that ensures the rejection of parameters at which an output signal lower than 850 V is generated.

Fig. 8 presents the result of the sought optimum solution for the dynamic characteristics of the instrument, according to the criterion set for the fitness function with such determined limits of the condenser values: $C_1 = [10^{-5}, 0.005]$ F; C_2, $C_3 = [10^{-7}, 0.005]$ F.

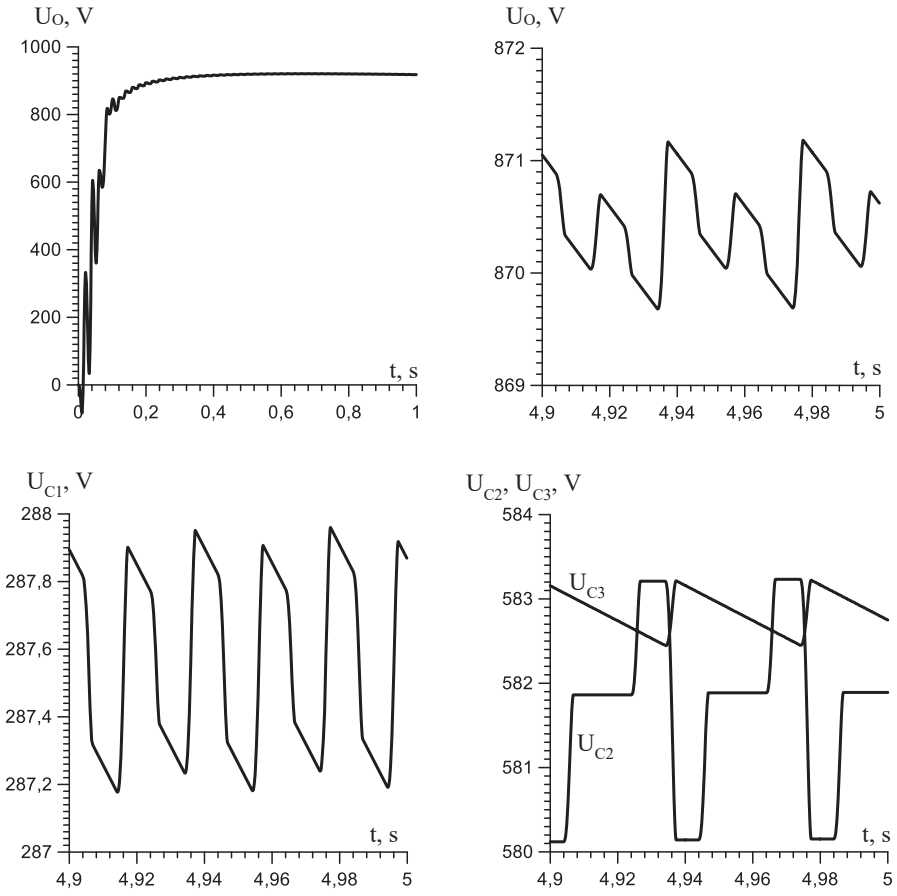

Fig. 8. Transient response of the voltage tripler with $R_O = 9000\ \Omega$, $C_1 = 4.986$ mF, $C_2 = 1.266$ mF, $C_3 = 4.654$ mF

The following settings were selected for the genetic algorithm: the population count was selected with chromosome 40 or 50; the probability of mutation was selected within the range of 5 to 15%; selective pressure coefficient was 1.7 or 1.8; chromosome 1 was selected for the elitism. The obtained characteristics in the fixed mode have quite a low pulse at a level of 1.57 V and a short time for returning to the operating mode. The only downside is the high value of the condenser capacity.

Fig. 9 presents the result of the search for the optimum value in the scale of condenser values C_1, C_2, C_3 = [10^{-7}, 0.0005] F. This means that at the beginning, the condenser capacity value was limited (restricted). Respectively, the dynamic characteristics of the instrument feature a smoother switch into the fixed mode and the pulse value in the fixed mode reaches 10.8 V.

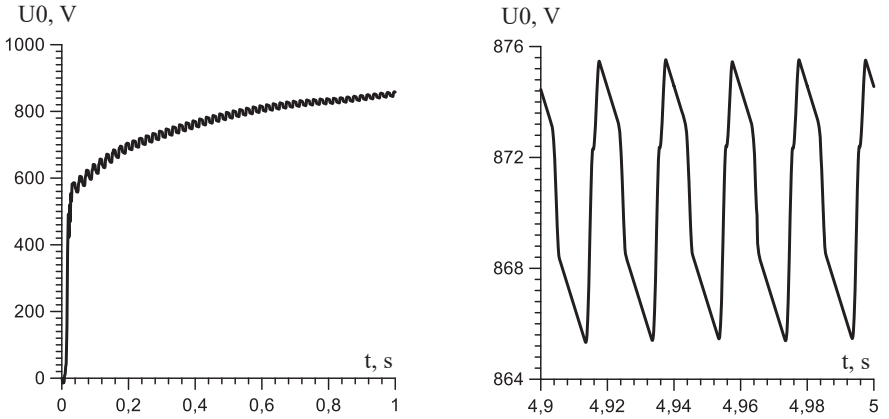

Fig. 9. Transient response of the voltage tripler with R_O = 9000 Ω, C_1 = 498.1 μF, C_2 = 24.42 μF, C_3 = 498.9 μF

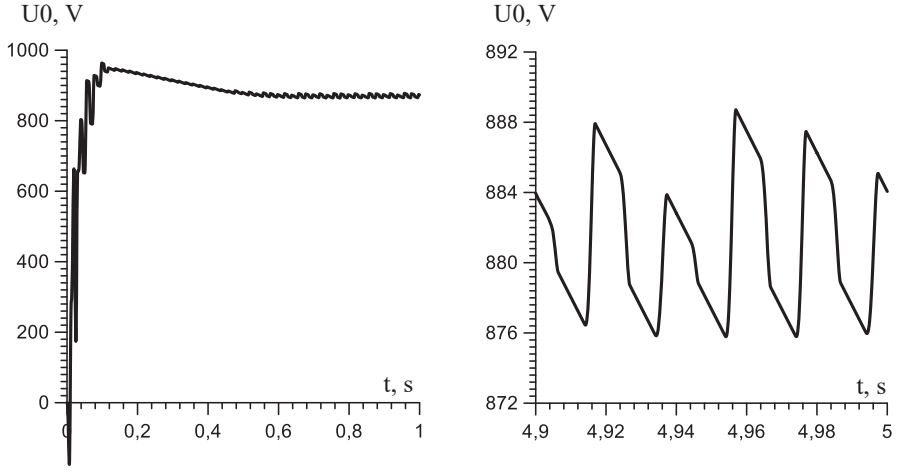

Fig. 10. Transient response of the voltage tripler with R_O = 5000 Ω, C_1 = 499.9 μF, C_2 = 252.9 μF, C_3 = 494.4 μF

It would also be interesting to investigate the operation of the instrument at a lower load resistance set at 5 κΩ (Fig. 10). The search for the optimum performance was performed at a condenser value scale of C_1, C_2, C_3 = [10^{-6}, 0.0005] F. The pulse value in the fixed mode was at a level of 13.6 V. In the case of lower values of the instrument load resistance, it was impossible to reach the strip value of 850 V.

6. Conclusion

Using the proposed mathematical model of the constant-to-variable voltage transducer with concurrent tripling of the amplitude, parameter optimisation of the instrument was performed. The condenser capacity values were selected by applying the classical genetic algorithm with the representation of genes by real digits. The conducted optimisation allowed the obtaining of good quality dynamic parameters of the instrument. The prepared mathematical model of the voltage tripler is universal and simple for algorithm setting.

References

[1] Choi Jae-Ho,Ji Jun-Keon, Park Min-Ho, *A novel voltage-regulated current controlled PWM-VSC converter with unity power factor*, Proceedings 14 Annual Conference of Industrial Electronics Society, Singapore, 24–28 October, 1988, 587–592.

[2] Kanaan H.Y., Al-Haddad K., Hayek A., Mougharbel I., *Design, study, modelling and control of a new single-phase high power factor rectifier based on the single-ended primary inductance converter and the Sheppard-Taylor topology*, IET Power Electronics, Vol. 2, Issue 2, 2009, 163–177.

[3] Kanaan H.Y., Al-Haddad K., Fadel M., *Modeling and control of a two-switch asymmetrical half-bridge Boost Power Factor Corrector for single-phase rectifiers*, IEEE 22nd International Symposium on Industrial Electronics, Taipei, Taiwan, 28–31 May, 2013, 1–6.

[4] Li Y., Junyent-Ferre A., Rodriguez-Bernuz J-M., *A Three-Phase Active Rectifier Topology for Bipolar DC Distribution*, IEEE Transactions on Power Electronics, V. PP, Issue 99, 2017, 1–1.

[5] Drozdowski P., Jeleń M., *Metoda eliminacji harmonicznych prądu przekształtnika sieciowego napędu trakcyjnego*, Technical Transactions, 1-E/2011, 53–65.

[6] Mazgaj W., Rozegnał B., Szular Z., *A novel soft switching system for three-phase voltage source inverter*, Technical Transactions, 2-E/2016, 3–15.

[7] Arias M., Fernández M., González D., Sebastián J., Balocco D., Diallo A., *Improving the design of the asymmetrical half-bridge converter without electrolytic capacitor for low-output-voltage ac-dc LED drivers*, IEEE Energy Conversion Congress and Exposition, NC, USA, 15–20 September, 2012, 3241–3248.

[8] Tarisciotti L., Zanchetta P., Watson A., Clare J.C., Degano M., Bifaretti S., *Modulated Model Predictive Control for a Three-Phase Active Rectifier*, IEEE Transactions on Industry Applications, Vol. 51, Issue 2, 2015, 1610–1620.

[9] Samotyy V., *Evolutionary optimization of DC motor control system*, Technical Transactions, 3-E/2016, 215–227.
[10] Sivanandam S.N., Deepa S.N., Introduction to Genetic Algorithms, Springer-Verlag Berlin Heidelberg, 2008.
[11] Randy L. Haupt, Sue Ellen Haupt, Practical genetic algorithms, 2nd ed., John Wiley & Sons, Inc., Hoboken, New Jersey, 2004.

If you want to quote this article, its proper bibliographic entry is as follow: Samotyy V., Dzelendzyak U., Pavelchak A., *An evolutionary model for the parametric optimisation of electromagnetic instruments of variable structures*, Technical Transactions, Vol. 4/2018, pp. 103–118.